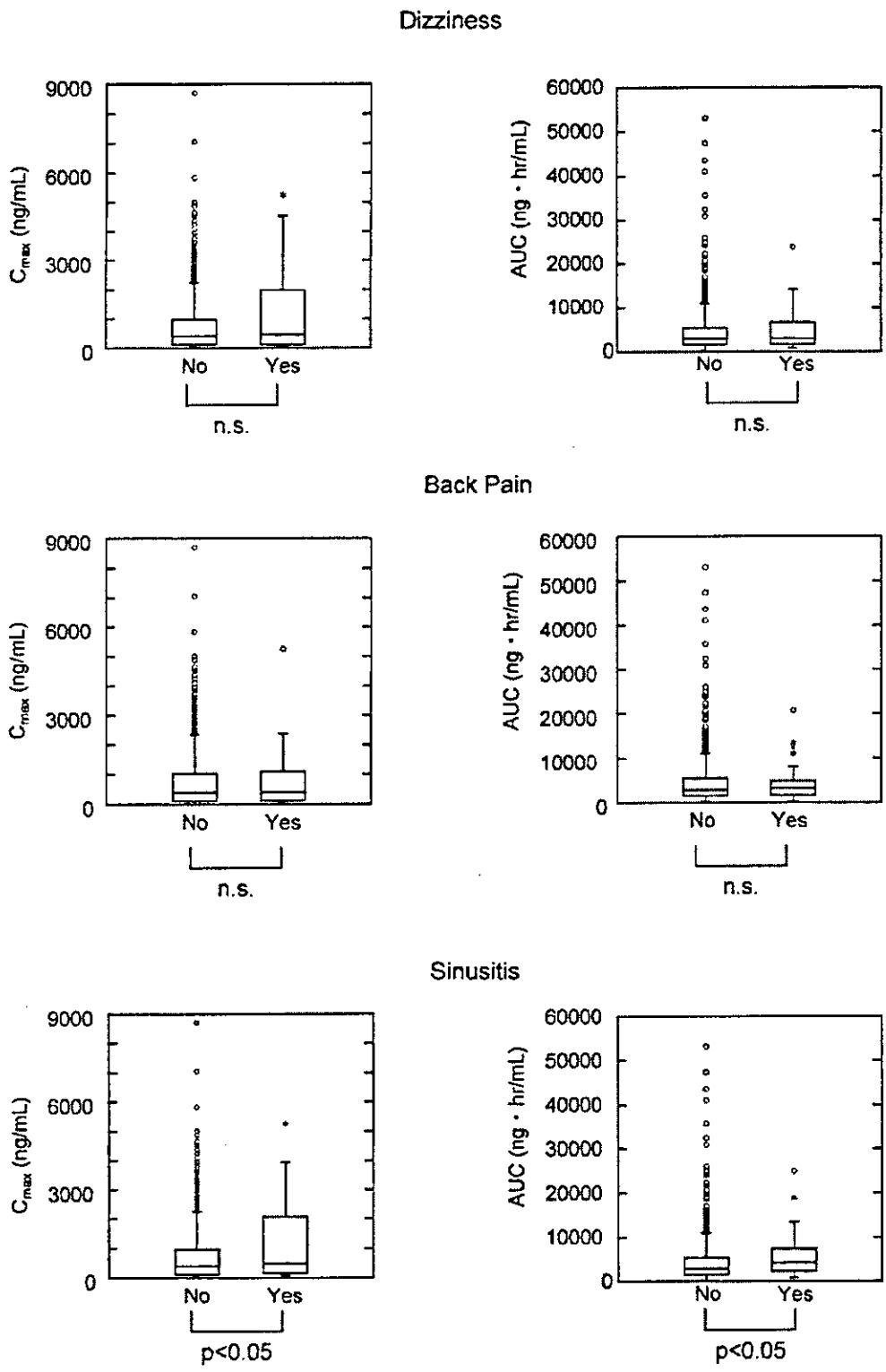
Dizziness
C_{max} (ng/mL)
9000
6000
3000
0
No
Yes
n.s.
AUC (ng・hr/mL)
60000
50000
40000
30000
20000
10000
0
No
Yes
n.s.
Back Pain
C_{max} (ng/mL)
9000
6000
3000
0
No
Yes
n.s.
AUC (ng・hr/mL)
60000
50000
40000
30000
20000
10000
0
No
Yes
n.s.
Sinusitis
C_{max} (ng/mL)
9000
6000
3000
0
No
Yes
p<0.05
AUC (ng・hr/mL)
60000
50000
40000
30000
20000
10000
0
No
Yes
p<0.05

Fig. 1(2)

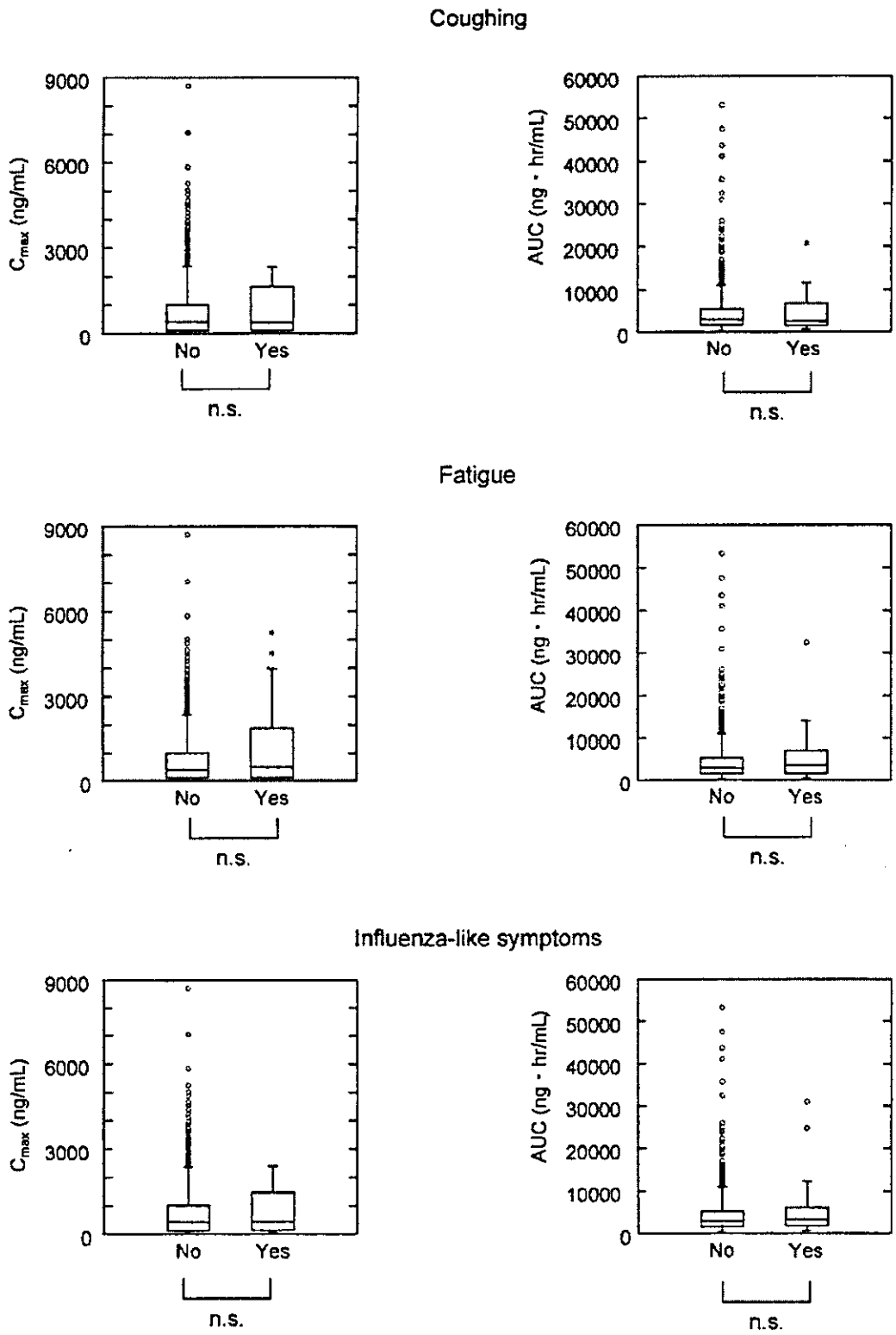
Coughing
C_{max} (ng/mL)
9000
6000
3000
0
No
Yes
n.s.
AUC (ng・hr/mL)
60000
50000
40000
30000
20000
10000
0
No
Yes
n.s.
Fatigue
C_{max} (ng/mL)
9000
6000
3000
0
No
Yes
n.s.
AUC (ng・hr/mL)
60000
50000
40000
30000
20000
10000
0
No
Yes
n.s.
Influenza-like symptoms
C_{max} (ng/mL)
9000
6000
3000
0
No
Yes
n.s.
AUC (ng・hr/mL)
60000
50000
40000
30000
20000
10000
0
No
Yes
n.s.

Fig. 1(3)

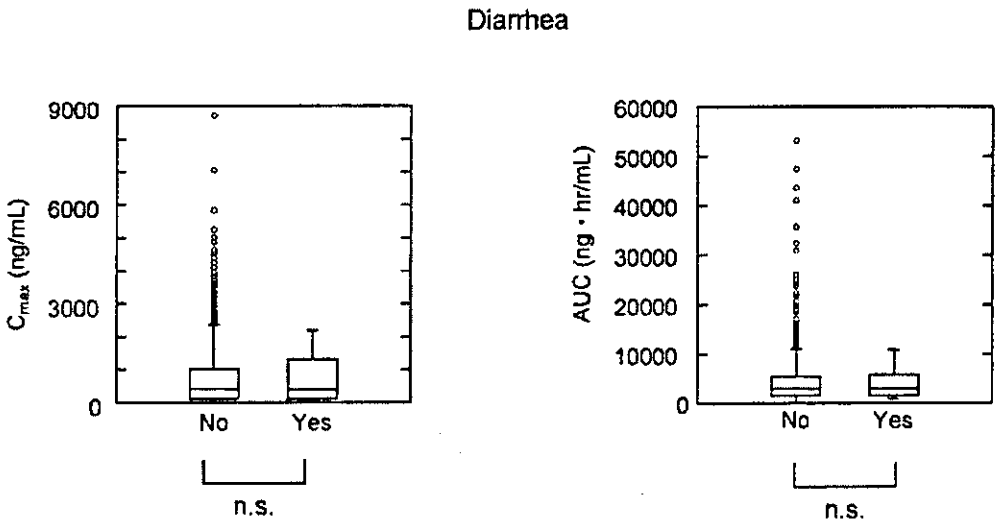

Fig. 1(4)

Fig. 1. The box plots of estimated C_{max} and AUC divided by occurrence of each adverse event.
The top, middle and bottom lines of each box correspond to the 75% (top quartile), 50% (median) and 25% (bottom quartile) values. The whiskers show the range of values that falls within 1.5 times the interquartile range and asterisks show values outside this. Open circles show values that exceed 3 times the interquartile range.
n.s.: not significant (Mann-Whitney test) $p<0.05$ (Mann-Whitney test)

Table 4. Occurrence of headache and observed C_{max} in the steady state

Observed C_{max} (ng/mL)		p value[a)]
no	yes	
971±1249 (112)	1214±1865 (16)	0.521

The numbers represent mean±S.D.
The numbers in parentheses represent numbers of subjects.
a) Mann-Whitney test

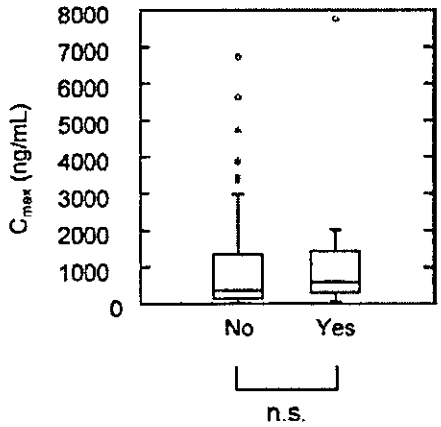

Fig. 2. The box plot of observed C_{max} divided by occurrence of headache.
The top, middle and bottom lines of each box correspond to the 75% (top quartile), 50% (median) and 25% (bottom quartile) values. The whiskers show the range of values that falls within 1.5 times the interquartile range and asterisks show values outside this. Open circles show values that exceed 3 times the interquartile range.
n.s.: not significant (Mann-Whitney test)

concentrations would have reached the steady state in these subjects. Therefore, pharmacokinetic parameters in the steady state were used in this study. Adverse events that occurred in the same subject at different dosages were counted separately, because the difference of exposure might affect the occurrence of adverse events. With regard to the co-administration of HCTZ, the previous PPK analysis[6] and the result of a clinical trial[12] revealed that HCTZ did not affect the pharmacokinetics of telmisartan, so the adverse events were not classified into groups with or without co-administration of HCTZ. In order to confirm the results of these analyses using C_{max} and AUC values calculated by the PPK model, observed C_{max} values were also used for analysis.

As shown in **Table 2**, the most frequent adverse event was headache, which occurred in 146 subjects. It was reported that headache was the most common adverse event in the pooled tolerability data.[8] Most of the top 10 adverse events in this study were the same as in the previous report,[8] suggesting that the adverse events analyzed in this study are common events for telmisartan. No significant between-group differences were observed in any pharmacokinetic parameter for eight out of the ten adverse events (**Table 3**), or in observed C_{max} (**Table 4**). The groups with and without serious adverse events showed no significant difference in pharmacokinetic parameters (**Table 6**). Although significant

Table 5. Reported serious adverse events in 8 trials performed in US and EU

Adverse Event	Number of subject
Myocardial infarction	3
Chest pain	3
Cardiac failure	3
Cerebrovascular disorder	2
Basal cell carcinoma	2
Arthritis aggravated	2
Angina pectoris	2
Prostatic disorder	1
Migraine	1
Adenocarcinoma NOS	1
Fibrillation atrial	1
Arthritis	1
Diverticulitis	1
Gastroenteritis	1
Dehydration	1
Neoplasm malignant	1
Abdominal pain	1
Cholecystitis	1
Fever	1
Pain	1
Tendon disorder	1
Drug dependence	1
Urethral disorder	1
Bundle branch block	1
Thrombophlebitis deep	1
Strabismus	1
Arthrosis	1
Pulmonary carcinoma	1
Circulatory failure	1
Tachycardia ventricular	1
Dyspepsia	1
Cholelithiasis	1
Pneumonia	1
Coughing	1
Dyspnoea	1

Subjects with more than one serious adverse event are included.

differences in pharmacokinetic parameters were observed for two events, pain and sinusitis, the intersubject variability of pharmacokinetic parameters was large and there were many subjects whose C_{max} and AUC were high, who experienced no adverse event (**Fig. 1**). Thus, there was no clear relationship between pharmacokinetic parameters and the occurrence of adverse events, or serious adverse events, and increase of exposure does not necessarily result in the occurrence of an adverse event. In this study, we considered adverse events from the viewpoint of safety assessment. In general, side effects are symptoms or physiological changes that result directly from the specific biological and pharmacological activity of the drug, and they tend to be dose-dependent and predictable. On the other hand, an adverse event is defined as any untoward medical occurrence during a clinical investigation in a subject administered a drug, and so it is not clear if adverse events result directly from the drug's pharmacological activity or not. Therefore, it seems better to analyze the relationship between side effects and exposure to a drug than that between adverse effects and exposure. However, we could not obtain enough data on side

Table 6. Occurrence of serious adverse events and estimated PK parameters in the steady state (C_{max} and AUC)

Serious adverse event	no	yes	p value[a)]
C_{max} (ng/mL)	745 ± 914 (1466)	628 ± 907 (34)	0.096
AUC (ng·hr/mL)	4241 ± 4354 (1466)	4787 ± 9125 (34)	0.147

The numbers represent mean ± S.D.
The numbers in parentheses represent numbers of subjects.
a) Mann-Whitney test

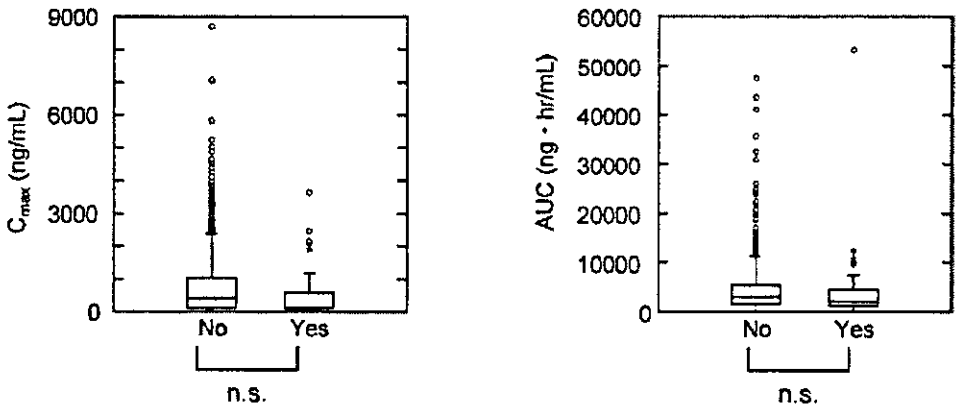

Fig. 3. The box plots of estimated C_{max} and AUC divided by occurrence of serious adverse events.
The top, middle and bottom lines of each box correspond to the 75% (top quartile), 50% (median) and 25% (bottom quartile) values. The whiskers show the range of values that falls within 1.5 times the interquartile range and asterisks show values outside this. Open circles show values that exceed 3 times the interquartile range.
n.s.: not significant (Mann-Whitney test)

effects for analysis, as telmisartan is well tolerated and the occurrence rate of side effects of telmisartan is low. Therefore, we investigated the relationship between the occurrence of adverse events and pharmacokinetic parameters.

In the previous report on the PPK model, the AUC and C_{max} in Japanese subjects were smaller than those in subjects included in the Europe and United States' clinical trials, mainly due to the difference of food condition.[6] The result of this study suggests that the difference of plasma concentrations between Japanese and other countries' clinical data does not have a marked effect on the occurrence of adverse events.

It has already been reported that angiotensin receptor blockers including telmisartan, are well tolerated and have a low incidence of adverse events, and the adverse event profile is often similar to that of placebo.[7] So it is reasonable that no clear relationship between pharmacokinetic parameters and the occurrence of adverse events was observed, even in 1194 subjects.

If more information about the relationship between side effects, not adverse events, and plasma concentrations were collected, it might prove useful to predict the occurrence of side effects from the plasma concentration.

In conclusion, the relationship between pharmacokinetic parameters of telmisartan and the occurrence of adverse events was investigated based on a total of 1500 cases from 8 clinical trials. For most of the adverse events, no significant difference in pharmacokinetic parameters between subjects with and without occurrence of adverse events was observed. Even in the case of adverse events that were found to have a significant difference, there were many subjects without any adverse event whose pharmacokinetic parameters were higher than those of subjects showing an adverse event. These results suggest that there is no clear relationship between pharmacokinetic parameters and the occurrence of adverse events.

References

1) Wienen, W., Hauel, N., Van Meel, J. C., Narr, B., Ries, U. and Entzeroth, M.: Pharmacological characterization of the novel nonpeptide angiotensin II receptor antagonist, BIBR 277. *Br. J. Pharmacol.*, **110**: 245–252 (1993).
2) Wienen, W., Entzeroth, M., Meel, J. C. A., Stangier, J., Busch, U., Ebner, T., Schmid, J., Lehmann, H., Matzek, K., Kempthorne-Rawson, J., Gladigau, V. and Hauel, N. H.: A review on telmisartan: a novel, long-acting angiotensin II-receptor antagonist. *Cardiovasc. Drug Rev.*, **18**: 127–156 (2000).
3) Neutel, J. M. and Smith, D. H. G.: Dose response and antihypertensive efficacy of the AT1 receptor antagonist telmisartan in patients with mild to moderate hypertension. *Adv. Ther.*, **15**: 206–217 (1998).
4) Smith, D. H. G., Matzek, K. M. and Kempthorne-Rawson, J.: Dose response and safety of telmisartan in patients with mild to moderate hypertension. *J. Clin. Pharmacol.*, **40**: 1380–1390 (2000).
5) Tatami, S., Sarashina, A., Yamamura, Y., Igarashi, T. and Tanigawara, Y.: Population pharmacokinetics of an angiotensin II receptor antagonist, telmisartan, in healthy volunteers and hypertensive patients. *Drug Metab. Pharmacokin.*, **18**: 203–211 (2003).
6) Tatami, S., Yamamura, Y., Sarashina, A., Yong, C. L., Igarashi, T. and Tanigawara, Y.: Pharmacokinetic comparison of an angiotensin II receptor antagonist, telmisartan, in Japanese and Western hypertensive patients using population pharmacokinetic method. *Drug Metab. Pharmacokin.*, **19**: 15–23 (2004).
7) Israili, Z. H.: Clinical pharmacokinetics of angiotensin II (AT1) receptor blockers in hypertension. *J. Hum. Hypertens.*, **14 Suppl 1**: S73–86 (2000).
8) Sharpe, M., Jarvis, B. and Goa, K. L.: Telmisartan: a review of its use in hypertension. *Drugs*, **61**: 1501–1529 (2001).
9) Karlberg, B. E., Lins, L. E. and Hermansson, K.: Efficacy and safety of telmisartan, a selective AT1 receptor antagonist, compared with enalapril in elderly patients with primary hypertension. TEES Study Group. *J. Hypertens.*, **17**: 293–302 (1999).
10) Hannedouche, T., Chanard, J. and Baumelou, B.: Evaluation of the safety and efficacy of telmisartan and enalapril, with the potential addition of frusemide, in moderate-renal failure patients with mild-to-moderate hypertension. *J. Renin. Angiotensin Aldosterone Syst*, **2**: 246–254 (2001).
11) Dunselman, P. H.: Effects of the replacement of the angiotensin converting enzyme inhibitor enalapril by the angiotensin II receptor blocker telmisartan in patients with congestive heart failure. The replacement of angiotensin converting enzyme inhibition (REPLACE) investigators. *Int. J. Cardiol.*, **77**: 131–138; discussion 139–140 (2001).
12) Yong, C. L., Dias, V. C. and Stangier, J.: Multiple-dose pharmacokinetics of telmisartan and of hydrochlorothiazide following concurrent administration in healthy subjects. *J. Clin. Pharmacol.*, **40**: 1323–1330 (2000).
13) Smith, D. H. G., Neutel, J. M. and Morgenstern, P.: Once-daily telmisartan compared with enalapril in the treatment of hypertension. *Adv. Ther.*, **15**: 229–240 (1998).
14) Neutel, J. M., Frishman, W. H., Oparil, S., Papademitriou, V. and Guthrie, G.: Comparison of telmisartan with lisinopril in patients with mild-to-moderate hypertension. *Am. J. Ther.*, **6**: 161–166 (1999).
15) Boeckmann, A. J., Sheiner, L. B. and Beal, S. L.: NONMEM users guide. NONMEM Project Group, University of California at San Francisco. (1998).
16) Stangier, J., Su, C. A. and Roth, W.: Pharmacokinetics of orally and intravenously administered telmisartan in healthy young and elderly volunteers and in hypertensive patients. *J. Int. Med. Res.*, **28**: 149–167 (2000).

Drug Metab. Pharmacokin. 19 (1): 15–23 (2004).

Regular Article

Pharmacokinetic Comparison of an Angiotensin II Receptor Antagonist, Telmisartan, in Japanese and Western Hypertensive Patients Using Population Pharmacokinetic Method

Shinji TATAMI[1], Norio YAMAMURA[1], Akiko SARASHINA[1], Chan-Loi YONG[2], Takashi IGARASHI[1] and Yusuke TANIGAWARA[3]

[1]*Department of Drug Metabolism and Pharmacokinetics, Kawanishi Pharma Research Institute, Nippon Boehringer Ingelheim Co., Ltd., Kawanishi, Japan*
[2]*Department of Drug Metabolism and Pharmacokinetics, Boehringer Ingelheim Pharmaceuticals Inc., CT, USA*
[3]*Department of Hospital Pharmacy, School of Medicine, Keio University, Tokyo, Japan*

Summary: The objectives of this study were to develop a population pharmacokinetic (PPK) model for telmisartan based on the pooled data obtained from the different racial populations and then to identify the factors that affect the pharmacokinetics of telmisartan for the comparison between the regions.

A PPK model was established based on the data of 1343 subjects in 12 clinical trials. The PK profiles of telmisartan were described with a 2-compartment model with first-order absorption. The obtained model could predict the observed plasma concentrations well. This PPK model suggested that CL/F was a function of age, dose, gender, race, alcohol consumption and liver function. A marked difference was observed in the plasma concentration profiles between Japanese and other countries' subjects. However, the effect of the factor "race" on CL/F was not large. In the present PPK model, "trial condition" affected all PK parameters except for V_2/F. The condition differences were in food condition and formulation (Japanese: fed, capsule, US and EU: fasted, tablet). The extent of difference in the plasma concentration profiles simulated for Japanese and Caucasian using the PPK model under the same demographic condition was comparable with the results of the food effect study performed previously in Japan. The findings suggest that the difference in the plasma concentration profiles between Japanese and other countries' subjects was mainly due to the difference of food intake conditions under which the clinical trials were performed.

Key words: population pharmacokinetics; NONMEM; angiotensin II receptor antagonist; telmisartan; bridging

Introduction

Telmisartan is a nonpeptide angiotensin II receptor antagonist,[1,2] used for the treatment of hypertension.[3,4] Several clinical trials on telmisartan have been performed in the United States (US) and European countries (EU). In Japan, several pharmacokinetic studies in healthy volunteers and hypertensive patients have been also performed.

Population pharmacokinetic (PPK) analysis has been applied not only to therapeutic drug monitoring, but also to the drug development process.[5] PPK analysis is helpful to identify the factors that affect the pharmacokinetics of a drug, or to explain variability in a target population.[6] We have established a PPK model based on the Japanese PK data.[7] The objectives of this trial were to develop a PPK model for telmisartan based on the large data set obtained in the Western countries and Japan, and to identify the factors that affect the pharmacokinetics of telmisartan for the comparison between these regions.

Methods

Subjects and trial design: Data were collected from 1343 subjects enrolled in 12 clinical trials. Four studies had been performed in Japan and the other eight in the US or EU. All subjects had received telmisartan orally. The details of the trials are summarized in **Table 1.**

Received; June 28, 2003, Accepted; December 4, 2003
To whom correspondence should be addressed: Shinji TATAMI, *Department of Drug Metabolism and Pharmacokinetics, Kawanishi Pharma Research Institute, Nippon Boehringer Ingelheim Co., Ltd., Kawanishi 666-0193, Japan. Tel. +81-72-790-2163, Fax. +81-72-793-1089, E-mail: tatami@boehringer-ingelheim.co.jp*

Table 1. Sources of plasma telmisartan concentration data collected in the clinical trials

	Trial No.	Subjects	Dose (mg)	Number of subjects	Number of measurements	Ref. No.
Japan	1	Healthy male volunteers	40	20	221	8
	2	Hypertensive patients[a]	40, 80	20	298	9
	3	Hypertensive patients with renal dysfunction[a]	40	19	263	10
	4	Hypertensive patients	20, 40, 80	90 (Total 149)	784 (Total 1566)	11
US & EU	5	Hypertensive patients[a]	40, 80, 120	117	1567	4
	6	Hypertensive patients	20, 40, 80, 120, 160	220	1342	3
	7	Hypertensive patients	40, 80, 120, 160	278	854	13
	8	Hypertensive patients	40, 80, 160	358	1298	12
	9	Elderly hypertensive patients	20, 40, 80	94	166	14
	10	Hypertensive patients with renal dysfunction	40, 80	9	27	15
	11	Stable chronic symptomatic congestive heart failure patients	10, 20, 40, 80	106	240	16
	12	Healthy volunteers	160	12 (Total 1194)	427 (Total 5921)	17

Administration of telmisartan was performed after food intake in the Japanese trials and before food intake in the US and EU trials.
a: Studies used for non-compartmental analysis.

1) Trials in Japan: Twenty healthy male subjects in a phase I trial received 40 mg of telmisartan (Trial No. 1).[8] The objective of this trial was to investigate the effect of food on the relative bioavailability. The 221 plasma concentrations obtained after food intake were included in the data set.

Hypertensive patients in the other three studies received 20, 40 or 80 mg of telmisartan after food intake. Trial No. 2 was performed in 20 essential hypertensive patients to obtain the pharmacokinetics of telmisartan at the dose of 40 or 80 mg for 14 days.[9] Trial No. 3 was performed in 19 hypertensive patients with renal dysfunction (SCr: 1.5 to 4.0 mg/dL) to evaluate the difference in their pharmacokinetics at the dose of 40 mg for 7 days.[10] Trial No. 4 was performed in 90 hypertensive patients to obtain the pharmacokinetic data after single administration of 20, 40 or 80 mg, with the objective of obtaining enough pharmacokinetic data to perform PPK analysis in Japanese patients.[11]

A total of 1566 concentration measurements from these four studies was collected.

2) Trials in the US and EU: Four studies (Trial No. 5, 6, 7 and 8) were performed in hypertensive patients. They received 20, 40, 80, 120 or 160 mg of telmisartan for 4–48 weeks.[3,4,12,13] Trial No. 9 was performed in 94 elderly hypertensive patients at the dose of 20, 40 or 80 mg for 26 weeks.[14] Trial No. 10 was a study in 9 hypertensive patients with renal disfunction (creatinine clearance: 20 to 70 mL/min) at the dose of 40 or 80 mg for 12 weeks.[15] Trial No. 11 was a study in 106 patients with stable chronic symptomatic congestive heart failure at the dose of 10, 20, 40 or 80 mg for 12 weeks.[16] A drug-drug interaction study (Trial No. 12) between telmisartan and hydrochlorothiazide (HCTZ) was included in this analysis. Twelve healthy subjects were administered 160 mg of telmisartan for 7 days.[17] Administrations of telmisartan in these 8 studies were performed before food intake. A total of 5921 concentration measurements from 1194 subjects were collected.

The demographic and physiopathological parameters are summarized in **Table 2.**

Determination of telmisartan in plasma: Concentration of telmisartan in plasma was determined by a validated HPLC-fluorescence assay using a column-switching technique. The limit of the quantification was 0.5 ng/mL (Trial No. 1–4, 9, 10 and 11) or 1.0 ng/mL (Trial No. 5–8 and 12).

Model development: A PPK model for telmisartan based on the Japanese trial data had been established prior to this analysis.[7] The data used for building the Japanese PPK model were combined with the data from the eight trials in the US and EU. Using these merged data, a PPK analysis for telmisartan was performed based on the Japanese PPK model as a starting model.

The PPK modeling was performed using the NONMEM program (double precision, version V, level 1.0) with its library subroutines ADVAN4 and TRANS4.[18] A two-compartment open model with first-order absorption was used for description of the PK profile. The basic PK parameters were oral clearance (CL/F, L/hr), volume of distribution for the central compartment (V_1/F, L), inter-compartmental clearance (Q/F, L/hr), volume of distribution for the peripheral compartment (V_2/F, L), first-order absorption rate constant (Ka, hr^{-1}) and absorption lag time (ALAG, hr). The first-

Table 2. Description of the population participating in the present study

		Japan		US+EU	
Gender	Male	107	(71.8%)	788	(66.0%)
	Female	42	(28.2%)	406	(34.0%)
Dose	10 mg	—	—	25	(2.1%)
	20 mg	31	(20.8%)	90	(7.5%)
	40 mg	78	(52.3%)	342	(28.6%)
	80 mg	40	(26.8%)	319	(26.7%)
	120 mg	—	—	151	(12.6%)
	160 mg	—	—	267	(22.4%)
Alcohol	Non-drinker	57	(38.3%)	523	(43.8%)
	Drinker	92	(61.7%)	671	(56.2%)
Race	White	—	—	930	(77.9%)
	Black	—	—	154	(12.9%)
	Hispanic	—	—	96	(8.0%)
	Others (including Japanese)	149	(100%)	14	(1.2%)
Smoking history	Non-smoker	63	(42.3%)	574	(48.1%)
	Ex-smoker	19	(12.8%)	395	(33.1%)
	Smoker	67	(45.0%)	225	(18.8%)
HCTZ co-administration	No	149	(100%)	994	(83.2%)
	Yes	—	—	200	(16.8%)
Age (year)		50.5±16.0 (20–77)		55.8±11.6 (19–86)	
Weight (kg)		63.9±13.0 (30.5–118.3)		86.7±18.1 (38.6–159.1)	
Serum creatinine (mg/dL)		1.22±0.74 (0.59–4.10)		0.91±0.28 (0.10–3.78)	
Glutamic-oxaloacetic transaminase (U)		22.5±12.9 (5–97)		22.5±10.1 (6–143)	
	≤60 U	145(97.3%)		1183(99.1%)	
	>60 U	4 (2.7%)		11 (0.9%)	

Categorical characteristics are given as number of patients, with percentage of total population in parentheses.
Continuous characteristics of patients are given as mean±S.D, with ranges in parentheses.

order estimation (FO) method was used.

The inter-individual variability for basic PK parameters was modeled by the log normal distribution, as described for CL/F as an example.

$$CL/F_j = TVCL \cdot \exp(\eta_{jCL/F})$$

where $\eta_{jCL/F}$ is a random variable that represents the difference between the true clearance of the j-th individual (CL/F_j) and the typical value (TVCL). The random variable $\eta_{jCL/F}$ is assumed to be normally distributed with the mean of zero and a variance of $\omega^2_{CL/F}$.

Residual variability was similarly modeled by the log normal distribution as follows:

$$C_{ij} = C_{pred,ij} \cdot \exp(\varepsilon_{ij})$$

where C_{ij} is the i-th observed plasma concentration of telmisartan for the j-th individual, $C_{pred,ij}$ is the concentration predicted by the PPK model, and ε_{ij} is a random intra-individual effect with zero mean and a variance of σ^2.

The minimum value of the NONMEM objective function (MOF) was used as a statistic to choose suitable models during the model-building process. Since the difference in MOF between one model and the other can be approximated as a χ^2 distribution with freedom of the number of parameter difference, a difference in MOF of 3.84 for 1 degree of freedom ($p<0.05$) was considered statistically significant in the model-building process.

Step 1; Initial population model based on merged data: The previously established PPK model for Japanese subjects[7] was as follows: CL/F was found to be associated with age, dose, and alcohol consumption. V_1/F was related to age and dose, and V_2/F was related to body weight and gender. Ka and ALAG were described as a function of dose.

In the present analysis, the data from the Japanese trials and the US and EU trials were merged. Telmisartan was administered orally before food intake in the US and EU trials using tablets or a capsule formulation. Both formulations were proven to be bioequivalent. On the other hand, all Japanese data used in this analysis were obtained with another capsule formulation after food intake. It was considered likely that such a difference in the trial conditions between Japan and other countries would affect the PK profile of telmisartan. Therefore, the factor "Trial" was incorporated into all the PK parameters in addition to the covariates in the Japanese PPK model to analyze the data comprehensively.

Step 2; Modeling of covariates: Additional factors, co-medication with HCTZ, race, gender, and liver function (GOT), were tested as covariates on CL/F. As for race, subjects were categorized into four groups, i.e., white, black, Hispanic and others including Japanese. Subjects were divided into two groups by GOT level as the marker of liver function. High GOT was defined as greater than 60 U of GOT. The full model was obtained after incorporation of the significant covariates.

Once we developed a full model which incorporated all possible covariates, each covariate was in tern examined by removing one by one to confirm the statistical significance (backward selection) using more stringent criterion of MOF of 6.63 ($p<0.01$). The final PPK model was obtained by preserving the significant covariates.

Non-compartmental analysis: Non-compartmental pharmacokinetic parameters (C_{max} and AUC) were calculated with a linear trapezoid rule using WinNonlin® professional software (version 3.1, Pharsight Corporation, Mountain View, CA) only for the subjects who had enough points of plasma concentration data. The trials used for analysis are marked in **Table 1**.

Model validation: Bootstrap resampling method was used to evaluate the stability of the final model.[19,20] The final PPK model was fitted repeatedly to the 200 additional bootstrap datasets. The mean of parameter estimates obtained calculated from the 200 bootstrap replications were compared with the final parameter estimates obtained from the original data set. Each pharmacokinetic parameter was logarithmically transformed to calculate 95% symmetric confidence intervals. These were then back-transformed.

Effect of covariates: In order to evaluate the effects of covariates on the plasma concentration of telmisartan, typical plasma profiles were predicted for various patient subgroups. These predictions were based on a two-compartment model with first-order absorption, using Excel® software.

Comparison of the simulated PK profiles for Japanese and Caucasian subjects: Based on average data of the demographics of the Japanese food-effect study,[8] the PK profiles were simulated for Japanese and Caucasian subjects. The demographic conditions for simulation were as follows: body weight: 62.9 kg, age: 22 years old, GOT: low, alcohol: drinker, gender: male. These conditions were same for both races. Race and trial condition were set respectively. The result of simulation was compared with that of Japanese food-effect study on the point of PK-profile differences.

Results

Demographic and clinical characteristics of the subjects are summarized in **Table 2**. A total of 1343 subjects (895 males and 448 females) were included in this analysis, and 7487 observations were used. The subjects' ages ranged from 19 to 86 years, body weight from 30.5 to 159.1 kg, and GOT from 5 to 143 U. These subjects had received 10, 20, 40, 80, 120 or 160 mg of telmisartan.

Step 1; Initial population model: The initial model, which is obtained by incorporation of the factor "Trial" into the Japanese PPK model established previously, is described by the following equations.

$$CL/F=\theta_{CL/F}\cdot AGE^{\theta_{CL/F}^{AGE}}\cdot DOSE^{\theta_{CL/F}^{DOSE}}\cdot\theta_{CL/F}^{\mathrm{Drinker}}\cdot\theta_{CL/F}^{TrialJ}\cdot e^{\eta_{CL/F}}$$

$$V_1/F=\theta_{V_1/F}\cdot AGE^{\theta_{V_1/F}^{AGE}}\cdot DOSE^{\theta_{V_1/F}^{DOSE}}\cdot\theta_{V_1/F}^{TrialJ}\cdot e^{\eta_{V_1/F}}$$

$$Q/F=\theta_{Q/F}\cdot\theta_{Q/F}^{TrialJ}\cdot e^{\eta_{Q/F}}$$

$$V_2/F=\theta_{V_2/F}\cdot WTKG^{\theta_{V_2/F}^{WTKG}}\cdot\theta_{V_2/F}^{Male}\cdot\theta_{V_2/F}^{TrialJ}\cdot e^{\eta_{V_2/F}}$$

$$Ka=\theta_{Ka}\cdot DOSE^{\theta_{Ka}^{DOSE}}\cdot\theta_{Ka}^{TrialJ}$$

$$ALAG=\theta_{ALAG}\cdot DOSE^{\theta_{ALAG}^{DOSE}}\cdot\theta_{ALAG}^{TrialJ}$$

where

AGE: age in years old
DOSE: dose in mg
WTKG: weight in kg
$\theta_{CL/F}^{\mathrm{Drinker}}$: 1 for non-drinker
$\theta_{V_2/F}^{Male}$: 1 for female
θ_{XXX}^{TrialJ}: 1 for US + EU trial

Step 2; Modeling of covariates: Co-medication with HCTZ, race, gender and liver function were tested as covariates on CL/F in addition to the basic model. Among the examined covariates, race, gender and liver function were found to affect CL/F. Gender was the most important covariate on CL/F (ΔMOF = 384.52) in this step of modeling. Race, gender and liver function were then combined in the following full model.

$$CL/F=\theta_{CL/F}\cdot AGE^{\theta_{CL/F}^{AGE}}\cdot DOSE^{\theta_{CL/F}^{DOSE}}\cdot\theta_{CL/F}^{\mathrm{Drinker}}\cdot\theta_{CL/F}^{Race}\times\theta_{CL/F}^{Male}\cdot\theta_{CL/F}^{High\_GOT}\cdot\theta_{CL/F}^{TrialJ}\cdot e^{\eta_{CL/F}}$$

$$V_1/F=\theta_{V_1/F}\cdot AGE^{\theta_{V_1/F}^{AGE}}\cdot DOSE^{\theta_{V_1/F}^{DOSE}}\cdot\theta_{V_1/F}^{TrialJ}\cdot e^{\eta_{V_1/F}}$$

$$Q/F=\theta_{Q/F}\cdot\theta_{Q/F}^{TrialJ}\cdot e^{\eta_{Q/F}}$$

$$V_2/F=\theta_{V_2/F}\cdot WTKG^{\theta_{V_2/F}^{WTKG}}\cdot\theta_{V_2/F}^{Male}\cdot\theta_{V_2/F}^{TrialJ}\cdot e^{\eta_{V_2/F}}$$

Table 3. Final PPK model

Population mean parameters		
CL/F	Clearance	$186 \times Age^{-0.386} \times Dose^{-0.233} \times \theta_{Gender1} \times \theta_{drinker} \times \theta_{Race} \times \theta_{GOT} \times \theta_{Trial1}$
V_1/F	Distribution volume of central compartment	$6400 \times Age^{-1.31} \times Dose^{-0.26} \times \theta_{Trial2}$
Q/F	Inter-compartmental clearance	$43.3 \times \theta_{Trial3}$
V_2/F	Distribution volume of peripheral compartment	$24.5 \times Weight^{0.829} \times \theta_{Gender2}$
Ka	First order absorption rate constant	$0.00087 \times Dose^{1.4} \times \theta_{Trial4}$
ALAG	Absorption lag time	$0.00208 \times Dose^{0.941} \times \theta_{Trial5}$
Inter-individual variability (CV%)		
$\omega_{CL/F}$	67.7%	
$\omega_{V_1/F}$	132.3%	
$\omega_{Q/F}$	101.0%	
$\omega_{V_2/F}$	218.9%	
Residual variability (CV%)		
σ^2	63.5%	

$\theta_{Gender1}$: 1.39 for male, 1 for female.
$\theta_{drinker}$: 1.21 for drinker, 1 for non-drinker.
θ_{Race}: 1 for white, 1.02 for black, 0.715 for Hispanic, and 0.932 for others (including Japanese).
θ_{GOT}: 0.357 for GOT > 60 U, 1 for GOT ≤ 60 U.
$\theta_{Gender2}$: 1.93 for male, 1 for female.
θ_{Trial1}: 1.74 for trials performed in Japan, 1 for trials performed in US+EU.
θ_{Trial2}: 12.1 for trials performed in Japan, 1 for trials performed in US+EU.
θ_{Trial3}: 2.06 for trials performed in Japan, 1 for trials performed in US+EU.
θ_{Trial4}: 2 for trials performed in Japan, 1 for trials performed in US+EU.
θ_{Trial5}: 6.18 for trials performed in Japan, 1 for trials performed in US+EU.

$$Ka = \theta_{Ka} \cdot DOSE^{\theta_{Ka}^{DOSE}} \cdot \theta_{Ka}^{TrialJ}$$

$$ALAG = \theta_{ALAG} \cdot DOSE^{\theta_{ALAG}^{DOSE}} \cdot \theta_{ALAG}^{TrialJ}$$

where

$\theta_{CL/F}^{Drinker}$: 1 for non-drinker
$\theta_{CL/F}^{Race}$: $\theta_{CL/F}^{white}$ for white, $\theta_{CL/F}^{black}$ for black, $\theta_{CL/F}^{Hispanic}$ for Hispanic, 1 for others including Japanese
$\theta_{CL/F}^{High\,GOT}$: 1 for low GOT subject
θ_{xxx}^{Male}: 1 for female
θ_{xxx}^{TrialJ}: 1 for US+EU trial

Model refinement was then made by the backward selection, in which statistically insignificant covariates were removed from the above full model. Preserving only statistically significant factors ($p<0.01$) led to the final PPK model. Through this process, the trial factor on V_2/F was removed from the full model. Therefore, the refined final PPK model is described by the following equations.

$$CL/F = \theta_{CL/F} \cdot AGE^{\theta_{CL/F}^{AGE}} \cdot DOSE^{\theta_{CL/F}^{DOSE}} \cdot \theta_{CL/F}^{Drinker} \cdot \theta_{CL/F}^{Race} \times \theta_{CL/F}^{Male} \cdot \theta_{CL/F}^{High\,GOT} \cdot \theta_{CL/F}^{TrialJ} \cdot e^{\eta_{CL/F}}$$

$$V_1/F = \theta_{V_1/F} \cdot AGE^{\theta_{V_1/F}^{AGE}} \cdot DOSE^{\theta_{V_1/F}^{DOSE}} \cdot \theta_{V_1/F}^{TrialJ} \cdot e^{\eta_{V_1/F}}$$

$$Q/F = \theta_{Q/F} \cdot \theta_{Q/F}^{TrialJ} \cdot e^{\eta_{Q/F}}$$

$$V_2/F = \theta_{V_2/F} \cdot WTKG^{\theta_{V_2/F}^{WTKG}} \cdot \theta_{V_2/F}^{Male} \cdot e^{\eta_{V_2/F}}$$

$$Ka = \theta_{Ka} \cdot DOSE^{\theta_{Ka}^{DOSE}} \cdot \theta_{Ka}^{TrialJ}$$

$$ALAG = \theta_{ALAG} \cdot DOSE^{\theta_{ALAG}^{DOSE}} \cdot \theta_{ALAG}^{TrialJ}$$

where

$\theta_{CL/F}^{Drinker}$: 1 for non-drinker
$\theta_{CL/F}^{Race}$: $\theta_{CL/F}^{white}$ for white, $\theta_{CL/F}^{black}$ for black, $\theta_{CL/F}^{Hispanic}$ for Hispanic, 1 for others including Japanese
$\theta_{CL/F}^{High\,GOT}$: 1 for low GOT subject
θ_{xxx}^{Male}: 1 for female
θ_{xxx}^{TrialJ}: 1 for US+EU trial

The PPK parameter estimates for the final model are summarized in **Table 3**.

Predictive ability and robustness of the final model: **Figure 1** shows the individual weighted residual plot for the final model. The individual weighted residuals were distributed around the zero value and no obvious tendency of over- or underestimation was observed, although there appeared to be a slight bias at low concentration.

For the subjects whose data points were enough to analyze the individual plasma concentration profile, C_{max} and AUC were calculated by two methods, PPK model prediction and non-compartmental analysis (**Fig. 2**). The scatter plots for C_{max} and AUC were around the line of identity.

The final PPK model was fitted repeatedly to the 200 additional bootstrap resampled data sets. All 200 estimation step were completed successfully and the results are summarized in **Table 4**. The geometric means of these 200 parameter estimates were within ±20% difference from the PPK parameters obtained with the original data set.

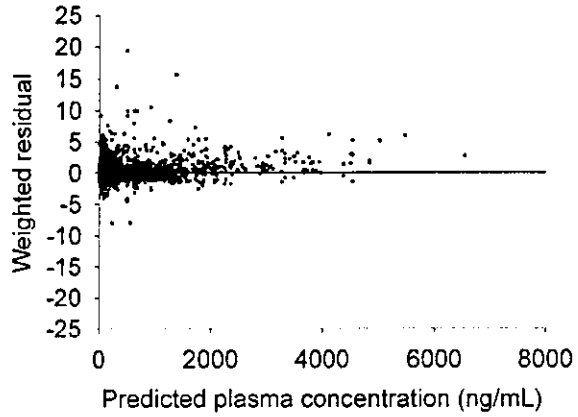

Fig. 1. The individual weighted residual plots for the predicted plasma concentration
The horizontal line represents the zero level.

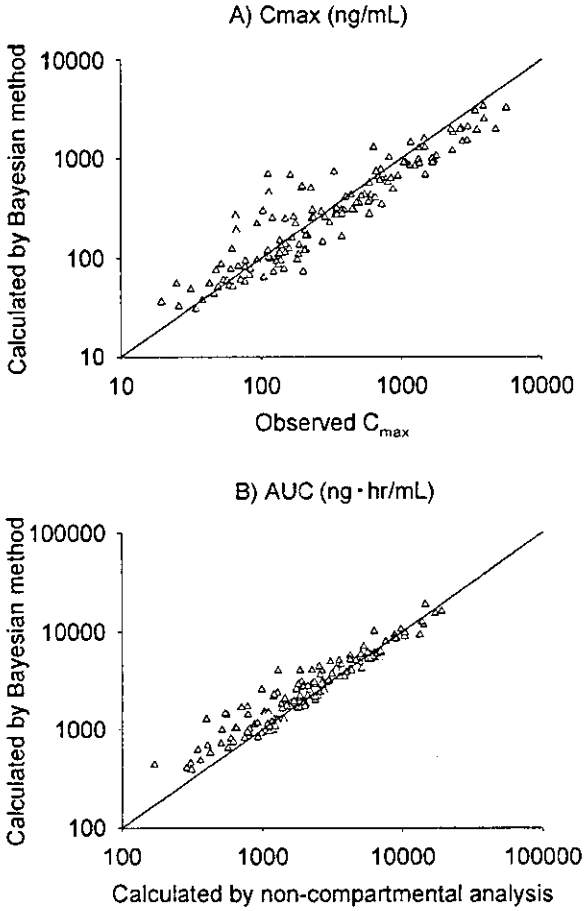

Fig. 2. Comparison of the pharmacokinetic parameters calculated by means of non-compartmental analysis and the PPK model
A) C_{max} and B) AUC. The line represents the line of identity.

Effect of covariates: The effect of each covariate on the plasma concentration of telmisartan was investigated. The pharmacokinetics of a typical subject, a 60 kg, 50-year-old, low GOT, male drinker administered 40 mg of telmisartan, was estimated using the population mean parameters of the final PPK model. Then, the change was investigated when each covariate was altered from the typical one. The pharmacokinetic parameters in a series of simulations are summarized for Japanese in **Table 5** and for Caucasian (white subjects) in **Table 6**. Plasma concentrations of females were simulated to be higher than those of males. The exposure increased with increasing age. Alcohol consumption increased exposure. High GOT decreased CL/F to about 36% of that of the low GOT group and C_{max} and AUC increased about 18% and 44% after the first dose in a typical Japanese subject. Dose affected CL/F, V_1/F, Ka and ALAG, and a super-proportional increase in exposure with dose was predicted, as shown in **Tables 5** and 6, rows 1, 6 and 7. Race was an influential covariate in CL/F, though a considerable change was predicted only in Hispanics (−28.5%) and there was no marked difference in Japanese (−6.8%) compared with white subjects.

Evaluation of difference in PK profiles of Japanese and non-Japanese subjects: **Figure 3** shows the result of simulation for Japanese and Caucasian on the same background. Compared with Caucasian, delayed t_{max} and lower C_{max} was simulated in Japanese. The ratios of C_{max} and AUC (Japanese/Caucasian) were 0.50 and 0.62, respectively. In the Japanese food-effect study, the ratios of C_{max} and AUC (fed/fasted) were 0.43 and 0.59, respectively.[8]

Discussion

The PPK model of telmisartan in healthy volunteers and hypertensive patients was based on a two-compartment model with first-order absorption. The CL/F was found to be associated with age, dose, gender, alcohol consumption, race and liver function, but not SCr or co-medication with HCTZ. Since the total urinary excretion of telmisartan was extremely low,[21] it is reasonable that CL/F was not affected by SCr, which indicates renal function, or co-medication with HCTZ, which is a diuretic. This result is consistent with the result of a clinical trial in subjects with mild to moderate renal dysfunction.[22] On the other hand, since telmisartan is mainly excreted via bile,[21,23,24] hepatic impairment was investigated as a potentially influential covariate. In the present analysis, GOT was used as a parameter of liver function. The results suggested that high GOT increased the exposure of telmisartan. Although patients with very high GOT were not included in the present data set, this supports the result of a previous clinical trial to compare the pharmacokinetics in healthy and hepatical-

Table 4. Summary of the bootstrap validation on the present population pharmacokinetic model and parameters for telmisartan

		Final estimates of the model parameters	Results of 200 bootstrap simulation		Bootstrap mean/final estimate ratio (%)
			Geometric mean	95% confidence interval lower-upper	
CL/F	[L/hr]	39.2	39.8	31.4–50.5	101.5
V_1/F	[L]	176.5	181.3	137.6–238.9	102.7
Q/F	[L/hr]	89.2	84.6	62.3–114.8	94.8
V_2/F	[L]	1409	1257	571–2770	89.3
Ka	[hr^{-1}]	0.304	0.303	0.238–0.386	99.6
Absorption lag time	[hr]	0.414	0.412	0.341–0.498	99.6
$\omega_{CL/F}$		0.458	0.461	0.359–0.591	100.6
$\omega_{V_1/F}$		1.75	1.60	0.85–2.99	91.2
$\omega_{Q/F}$		1.02	1.02	0.63–1.64	99.9
$\omega_{V_2/F}$		4.79	3.95	1.58–9.84	82.4
σ^2		0.403	0.390	0.319–0.476	96.7

PK parameters were simulated under following condition: 60 kg, 50 years old, low GOT, male non-drinker, 40 mg dose in Japanese trial.

Table 5. Influences of covariates on pharmacokinetic parameters in Japanese subjects

	Covariate						Estimated parameters						Calculated exposures	
Model No.	Gender	Weight (kg)	Age (year)	Drinker	Dose (mg)	GOT	CL/F (L/hr)	V_1/F (L)	Q/F (L/hr)	V_2/F (L)	Ka (hr^{-1})	Absorption lag time (hr)	C_{max} (ng/mL)	$AUC_{0\text{-}24hr}$ (ng·hr/mL)
1)	Male	60	50	Yes	40	low	47	177	89	1409	0.30	0.41	50	462
2)	Female	60	50	Yes	40	low	34	177	89	730	0.30	0.41	55	667
3)	Male	80	50	Yes	40	low	47	177	89	1788	0.30	0.41	50	432
4)	Male	60	70	Yes	40	low	42	114	89	1409	0.30	0.41	59	503
5)	Male	60	50	No	40	low	39	177	89	1409	0.30	0.41	52	505
6)	Male	60	50	Yes	20	low	56	211	89	1409	0.12	0.22	12	183
7)	Male	60	50	Yes	80	low	40	147	89	1409	0.80	0.79	193	1039
8)	Male	60	50	Yes	40	high	17	177	89	1409	0.30	0.41	59	666

The underline represents the covariate changed from model No. 1.
GOT: low and high represent less than and greater than 60 U, respectively.

Table 6. Influence of covariates on pharmacokinetic parameters in US+EU white subjects

	Covariate						Estimated parameters						Calculated exposures	
Model No.	Gender	Weight (kg)	Age (year)	Drinker	Dose (mg)	GOT	CL/F (L/hr)	V_1/F (L)	Q/F (L/hr)	V_2/F (L)	Ka (hr^{-1})	Absorption lag time (hr)	C_{max} (ng/mL)	$AUC_{0\text{-}24hr}$ (ng·hr/mL)
1)	Male	60	50	Yes	40	low	29	15	43	1409	0.15	0.07	76	690
2)	Female	60	50	Yes	40	low	21	15	43	730	0.15	0.07	85	957
3)	Male	80	50	Yes	40	low	29	15	43	1788	0.15	0.07	76	661
4)	Male	60	70	Yes	40	low	26	9	43	1409	0.15	0.07	82	737
5)	Male	60	50	No	40	low	24	15	43	1409	0.15	0.07	81	757
6)	Male	60	50	Yes	20	low	34	17	43	1409	0.06	0.03	14	234
7)	Male	60	50	Yes	80	low	25	12	43	1409	0.40	0.13	385	1600
8)	Male	60	50	Yes	40	high	10	15	43	1409	0.15	0.07	100	1018

The underline represents the covariate changed from model No. 1.
GOT: low and high represent less than and greater than 60 U, respectively.

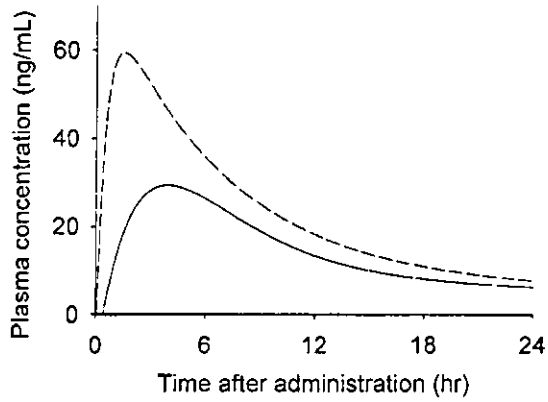

Fig. 3. Plasma concentration profiles
Simulated profile for the average demographic profile in the Japanese food effect study, a 62.9 kg, 22-year-old, low GOT, male drinker. The dashed line represents the profile based on white subjects in the US and EU trials and the solid line is that based on Japanese subjects in the Japanese trials.

ly impaired subjects, showing a marked difference in the pharmacokinetics of telmisartan in the two groups. In that trial, C_{max} and AUC of hepatically impaired subjects were higher than those of healthy subjects.[25]

Dose affected a few parameters besides CL/F. With increasing dose, CL/F and V_1/F decreased and Ka increased. The relationship between dose and these parameters is consistent with the super-proportional increase in the plasma concentration of telmisartan, which was observed in several clinical trials.[2,22,26] It is considered that the super-proportional increase of exposure is a consequence of saturable intestinal first-pass metabolism and high-affinity but limited-capacity uptake of telmisartan by the liver.[2] These complex features might be associated with the high inter-individual variability of telmisartan pharmacokinetics. The inter-individual variability of parameters in this PPK model was relatively high even after the fixed effects were incorporated into the model, and there might be other covariates.

Comparison of C_{max} and AUC obtained by non-compartmental analysis and PPK model prediction suggested that the final model could predict the PK profile of telmisartan well. In addition, bootstrap validation indicated that the final model was stable. Bootstrapping, which is an internal validation method, can be especially useful for evaluating the reliability of a population model.[20]

Using the present PPK model, the simulation for the typical subject, a 60 kg, 50-year-old, low GOT, male drinker, indicated that there was a great difference in the plasma concentration profiles between Japanese and white subjects (**Tables 5** and **6**).

The factor "race" between Japanese and white subjects does not greatly affect CL/F. The difference in the trial condition was considered to be the major cause of this discrepancy. The US and EU trails were conducted with oral administration before food intake. On the other hand, the Japanese trials were performed after food intake. In addition, different formulations were used in Japan and other countries. According to the food effect study conducted in Japan, food intake delayed t_{max} and reduced C_{max}. The ratios of C_{max} and AUC in the fed condition to those in the fasted condition were 0.43 and 0.59, respectively. A similar tendency was also observed in the simulated PK profile between Japanese and Caucasian, as shown in **Fig. 3**. This simulation was based on the average demographics of the Japanese food effect study, and then trial difference was simulated between Japanese and Caucasian under the same conditions of other factors. The ratios of C_{max} and AUC of Japanese to those of Caucasian were 0.50 and 0.62, showing similar results observed in the Japanese food effect study. This suggests that the difference in the plasma concentration between Japanese and other countries' subjects was mainly due to the food condition of trials.

In this analysis, a PPK model for telmisartan was developed. The model had good predictive ability and robustness. There was a large difference in plasma concentration profiles between clinical trials performed in Japan and in other countries. The main reason for this difference seems to be not a racial difference, but the difference in fed status at the time of telmisartan administration (before or after food). It is important to investigate the cause of difference in PK and then to evaluate how much impact the difference makes on the efficacy and safety of the drug in order to evaluate the clinical data from different regions (for "Bridging").

References

1) Wienen, W., Hauel, N., Van Meel, J. C., Narr, B., Ries, U. and Entzeroth, M.: Pharmacological characterization of the novel nonpeptide angiotensin II receptor antagonist, BIBR 277. *Br. J. Pharmacol.*, **110**: 245–252 (1993).
2) Wienen, W., Entzeroth, M., Meel, J. C. A., Stangier, J., Busch, U., Ebner, T., Schmid, J., Lehmann, H., Matzek, K., Kempthorne-Rawson, J., Gladigau, V. and Hauel, N. H.: A review on telmisartan: a novel, long-acting angiotensin II-receptor antagonist. *Cardiovasc. Drug Rev.*, **18**: 127–156 (2000).
3) Neutel, J. M. and Smith, D. H. G.: Dose response and antihypertensive efficacy of the AT1 receptor antagonist telmisartan in patients with mild to moderate hypertension. *Adv. Ther.*, **15**: 206–217 (1998).
4) Smith, D. H. G., Matzek, K. M. and Kempthorne-Rawson, J.: Dose response and safety of telmisartan in patients with mild to moderate hypertension. *J. Clin. Pharmacol.*, **40**: 1380–1390 (2000).
5) Williams, P. J. and Ette, E. I.: The role of population

pharmacokinetics in drug development in light of the Food and Drug Administration's 'Guidance for industry: population pharmacokinetics'. *Clin. Pharmacokinet.*, **39**: 385–395 (2000).
6) FDA: Guidance for industry: population pharmacokinetics. (1999).
7) Tatami, S., Sarashina, A., Yamamura, N., Igarashi, T. and Tanigawara, Y.: Population pharmacokinetics of an angiotensin II receptor antagonist, telmisartan, in healthy volunteers and hypertensive patients. *Drug Metab. Pharmacokin.*, **18**: 203–211 (2003).
8) Irie, S., Ogihara, T. and Tatami, S.: Influence of food on the bioavailability of single oral dose of BIBR277 (Telmisartan). *Jpn. Pharmacol. Ther.*, **30**: S201–208 (2002).
9) Ogihara, T., Takaori, A., Taki, C., Asai, Y., Yajima, K., Fukuda, H. and Tatami, S.: Pharmacokinetics of BIBR277 (Telmisartan) in patients with essential hypertension. *Jpn. Pharmacol. Ther. (in Japanese)*, **30**: S235–251 (2002).
10) Ogihara, T., Sakai, R., Fujita, Y., Shinko, S., Azekura, H., Obayashi, T., Tsuruta, Y. and Tatami, S.: Pharmacokinetics of BIBR277 (Telmisartan) in hypertensive patients with renal insufficiency. *Jpn. Pharmacol. Ther. (in Japanese)*, **30**: S183–199 (2002).
11) Ogihara, T., Minami, F., Kainuma, H., Asai, Y., Okada, Y., Fukuyo, K., Nakamura, Y., Osaka, A. and Tatami, S.: Pharmacokinetic evaluation of an angiotensin II AT1 receptor antagonist, BIBR277 (Telmisartan) in hypertensive patients. *Jpn. Pharmacol. Ther. (in Japanese)*, **30**: S271–283 (2002).
12) Neutel, J. M., Frishman, W. H., Oparil, S., Papademitriou, V. and Guthrie, G.: Comparison of telmisartan with lisinopril in patients with mild-to-moderate hypertension. *Am. J. Ther.*, **6**: 161–166 (1999).
13) Smith, D. H. G., Neutel, J. M. and Morgenstern, P.: Once-daily telmisartan compared with enalapril in the treatment of hypertension. *Adv. Ther.*, **15**: 229–240 (1998).
14) Karlberg, B. E., Lins, L. E. and Hermansson, K.: Efficacy and safety of telmisartan, a selective AT1 receptor antagonist, compared with enalapril in elderly patients with primary hypertension. TEES Study Group. *J. Hypertens.*, **17**: 293–302 (1999).
15) Hannedouche, T., Chanard, J. and Baumelou, B.: Evaluation of the safety and efficacy of telmisartan and enalapril, with the potential addition of frusemide, in moderate-renal failure patients with mild-to-moderate hypertension. *J. Renin. Angiotensin Aldosterone Syst.*, **2**: 246–254 (2001).
16) Dunselman, P. H.: Effects of the replacement of the angiotensin converting enzyme inhibitor enalapril by the angiotensin II receptor blocker telmisartan in patients with congestive heart failure. The replacement of angiotensin converting enzyme inhibition (REPLACE) investigators. *Int. J. Cardiol.*, **77**: 131–138; discussion 139–140 (2001).
17) Yong, C. L., Dias, V. C. and Stangier, J.: Multiple-dose pharmacokinetics of telmisartan and of hydrochlorothiazide following concurrent administration in healthy subjects. *J. Clin. Pharmacol.*, **40**: 1323–1330 (2000).
18) Boeckmann, A. J., Sheiner, L. B. and Beal, S. L.: NONMEM users guide. NONMEM Project Group, University of California at San Francisco (1998).
19) Parke, J., Holford, N. H. and Charles, B. G.: A procedure for generating bootstrap samples for the validation of nonlinear mixed-effects population models. *Comput. Methods Programs Biomed.*, **59**: 19–29 (1999).
20) Ette, E. I.: Stability and performance of a population pharmacokinetic model. *J. Clin. Pharmacol.*, **37**: 486–495 (1997).
21) Stangier, J., Schmid, J., Turck, D., Switek, H., Verhagen, A., Peeters, P. A., van Marle, S. P., Tamminga, W. J., Sollie, F. A. and Jonkman, J. H.: Absorption, metabolism, and excretion of intravenously and orally administered [^{14}C]telmisartan in healthy volunteers. *J. Clin. Pharmacol.*, **40**: 1312–1322 (2000).
22) Israili, Z. H.: Clinical pharmacokinetics of angiotensin II (AT1) receptor blockers in hypertension. *J. Hum. Hypertens.*, **14 Suppl 1**: S73–86 (2000).
23) Schmid, J., Beschke, K., Prox, A., Ebner, T., Busch, U., Koebe, H. G., Pahernik, S. and Schildberg, F. W.: *In vivo* and *in vitro* biotransformation of telmisartan, human hepatocyte cultures as an aid in human metabolic studies. *Exp. Toxicol. Pathol.*, **48**: 387 (1996).
24) Sharpe, M., Jarvis, B. and Goa, K. L.: Telmisartan: a review of its use in hypertension. *Drugs*, **61**: 1501–1529 (2001).
25) Stangier, J., Su, C. A., Schondorfer, G. and Roth, W.: Pharmacokinetics and safety of intravenous and oral telmisartan 20 mg and 120 mg in subjects with hepatic impairment compared with healthy volunteers. *J. Clin. Pharmacol.*, **40**: 1355–1364 (2000).
26) Stangier, J., Su, C. A. and Roth, W.: Pharmacokinetics of orally and intravenously administered telmisartan in healthy young and elderly volunteers and in hypertensive patients. *J. Int. Med. Res.*, **28**: 149–167 (2000).

Congenital Anomalies 2004; **44**, 18–26

ORIGINAL ARTICLE

Position-specific expression of *Hox* genes along the gastrointestinal tract

Naohisa Yahagi[1], Rika Kosaki[1,2], Taichi Ito[1], Takayuki Mitsuhashi[1], Hiroyuki Shimada[1], Masaru Tomita[3], Takao Takahashi[1], and Kenjiro Kosaki[1]

[1]Department of Pediatrics, Keio University School of Medicine, Tokyo, [2]Division of Medical Genetics, Saitama Children's Medical Center, Saitama, and [3]Laboratory for Bioinformatics, Keio University, Fujisawa, Japan

ABSTRACT ***Hox* genes play a critical role in morphogenesis of the early embryo along the anteroposterior axis. In mammals, 39 *Hox* genes with extensive homology are organized into 13 paralogous groups, forming four clusters on four separate chromosomes. The genes within each cluster are arranged in a 3′ to 5′ direction and expressed in a temporally and spatially coordinated manner along the anteroposterior axis in the vertebrae, limbs and viscera, including the gastrointestinal tract, but little is known about their spatial expression in the adult gastrointestinal tract. We used the quantitative polymerase chain reaction (PCR) intercalater method with SYBR Green™ to quantify human *Hox* gene expression in the adult gastrointestinal tract tissue: esophagus, stomach, duodenum, jejunum, ileum, ileocecum, cecum, ascending colon, transverse colon, descending colon and rectum. *Hox* gene expression was normalized to glyceraldehyde-3-phosphate-dehydrogenase (GAPDH) gene expression. The spatial expression pattern was analyzed by the multivariate method. The expression level of all 39 *Hox* genes could be measured in a reproducible manner. Genes with higher expression in the foregut-derived segments tended to have lower expression in hindgut-derived segments, whereas those with low expression in the former tended to have higher in the latter. Principal components analysis and permax analysis revealed a position-specific expression pattern of *Hox* genes along the anteroposterior axis of the adult gastrointestinal tract. The pattern recapitulates the expression pattern in the embryonic gastrointestinal tract. We suggest that *Hox* genes may play a pivotal role in the position-specific regenerative process of intestinal epithelial cells.**

Correspondence: Kenjiro Kosaki, MD, PhD, FACMG, Department of Pediatrics, Keio University School of Medicine, 35 Shinanomachi, Shinjuku-ku, Tokyo 160-8582, Japan. E-mail: kkosaki@sc.itc.keio.ac.jp

Received August 28, 2003; revised and accepted September 24, 2003.

Key Words: denaturing high-performance liquid chromatography, gastrointestinal tract, *Hox* genes, real-time polymerase chain reaction

INTRODUCTION

The *Hox* gene family consists of highly conserved transcription factors that specify the identity of body segments along the anteroposterior axis of the embryo. Since the discovery of the first prototypic *Hox* gene, *Antennapedia*, in *Drosophila* (McGinnis *et al.* 1984), homologous genes have been found in the genomes of a variety of animals (McGinnis & Krumlauf 1992). *Hox* genes arose from a common ancestral gene, duplicating several folds during evolution and forming a cluster in which homologous genes were arranged in tandem. Successive duplications of the cluster have given rise to the four *Hox* clusters in the vertebrate genome. Based on the sequence similarity of the *Hox* genes on separate clusters, *Hox* genes have been assigned to 13 groups referred to as 'paralogs' (Scott 1992). A subset of paralogs was lost within each cluster, leaving 39 *Hox* genes in the present mammalian genome.

Hox genes are expressed in a nested pattern along the anteroposterior axis of embryos and their expression pattern reflects their relative location within the cluster. Coordinated expression of *Hox* genes is critical to the development of clearly segmented structures, such as the vertebral column (Pollock *et al.* 1992), branchial arches (Hunt *et al.* 1991; Hunt *et al.* 1995) and limbs (Yokouchi *et al.* 1991). *Hox* genes are essential for regional specification of internal tubular organs, such as the gastrointestinal (GI) tract (Roberts *et al.* 1995; Roberts *et al.* 1998) and the genitourinary tract (Favier & Dolle 1997), along the anteroposterior axis. Yokouchi *et al.* (1995a) and Roberts *et al.* (1995) reported region-specific expression boundaries of paralogous groups 9–13 along the midgut and hindgut in chickens, and Kawazoe *et al.* (2002) demonstrated a region-specific expression

pattern of the *Hox* code in the foregut, midgut and hindgut in the developing gut of mice.

Targeted disruption of *Hox* genes in mice results in so-called 'homeotic' defects due to mis-specification of body segments along the anteroposterior axis of the central nervous system, axial skeleton, limbs, gut, urogenital tract and external genitalia. The critical role of *Hox* genes in morphogenesis has been further reflected in their abnormal expression patterns in embryos exposed to teratogens, including brief hyperthermia, valproic acid and hyperthermia, and in the presence of maternal diabetes. Faiella *et al.* (2000) documented homeotic mutations after prenatal exposure to valproic acid in mice and abnormal *Hox* gene expression in pluripotent embryonal carcinoma cells after treatment with valproic acid. Li & Shiota 1999) showed that heat treatment induced embryonic day-specific vertebral transformations accompanied by altered expression of *Hox* genes. Jacobs *et al.* (1998) demonstrated abnormal *Hox* expression in the lungs of fetuses from streptozotocin-treated rats.

Systematic and quantitative analysis of the *Hox* gene expression profile will be essential for further delineation of the homeotic potential of various teratogens. The purpose of the present study was twofold: first, to develop a comprehensive PCR-based system for simultaneous quantification of the expression levels of all 39 *Hox* genes by using information on their genome structure (Kosaki *et al.* 2002); and, second, to characterize the overall *Hox* expression pattern in the adult GI tract by means of multivariate analysis.

We chose to develop a real-time PCR-based system because of its sensitivity and specificity, which allows measurement of mRNA expression in small amounts of tissue (Gibson *et al.* 1996; Heid *et al.* 1996). The critical step in developing a reproducible real-time PCR-based system includes preparation of a highly purified standard template that is precisely quantified (Steuerwald *et al.* 2000). In the present study this step was accomplished by using a denaturing high-performance liquid chromatography (DHPLC) system for the preparation and quantification of the standard template (Kosaki *et al.* 2001).

METHODS

Primer design

Based on the complete genome structure of the human *Hox* genes which we recently determined (Kosaki *et al.* 2001), the primers for PCR analysis (Table 1) were designed to meet the following criteria: (1) The estimated annealing temperature is in the 55–62°C range predicted by the equation $T = 59.9°C + 0.41 \times (\%GC) - 600/length$. (2) Length is shorter than 300 bp (Calvo *et al.* 2000), so that the primer pairs are incapable of dimerization. (3) The 3′ end of the primers does not form a hairpin structure (<3 bp). (4) The 3′ end of the primers contains G or C residue (so-called 'GC clamp').

Amplification of the cDNA of the 39 *Hox* genes

Each of the 39 *Hox* genes was PCR-amplified from first-strand complementary DNA (cDNA) prepared from various human tissues (Multiple Tissue cDNA [MTC] panel, BD Biosciences Clontech, Palo Alto, CA, USA). The sources of the tissues or cells used for each of the *Hox* genes are listed in Table 2. An amplification reaction was carried out in a 20 μL volume containing the template DNA, 10 × reaction buffer, 200 mM dNTP mix, 1.5 mM $MgCl_2$, 10 pM of each primer, and 0.25 U Platinum *Taq* polymerase (Invitrogen, Carlsbad, CA, USA). Amplification conditions were: denaturation at 94°C for 10 min, followed by 40 cycles of 94°C for 60 s, 55–62°C for 60 s and 72°C for 60 s, and a final extension step of 72°C for 10 min (MJ RESEARCH, Waltham, MA, USA).

Purification of PCR product using DHPLC

The PCR products obtained as described in the previous section were purified and quantified by using the DHPLC system. DHPLC, ion-pair reverse-phase liquid chromatography in a column containing alkylated non-porous particles (Liu *et al.* 1998), was performed using the WAVE DNA Fragment Analysis system (Transgenomic, Omaha, NE, USA). A 100 μL sample of the PCR product was quantified with a UV detector at an excitation wavelength of 260 nm, and DNA chromatography was performed with buffers A (0.1 M Triethylammonium Acetate [TEAA]) and B (0.1 M TEAA in 25% acetonitrile) at a flow rate of 0.9 mL/min. A linear gradient from 52 to 62% buffer B over 10 min at a column temperature of 50°C was used. The extract was collected with the fraction collector unit. Areas under the curve (AUC) of the peaks corresponding to the PCR product were measured and converted to molar concentrations. Measured quantities of the purified PCR products were used as the template for real-time PCR.

Real-time PCR analysis

The PCR products quantified as described in the previous section were used in the subsequent real-time quantitative PCR reaction on a Cepheid Smart Cycler System (Cepheid, Sunnyvale, CA, USA) using the SYBR Green PCR kit as recommended by the manufacturer. Each reaction contained 2.5 μL of a 1 : 2500 dilution of SYBR Green buffer, 5 pM each primer, 0.4 mM each dNTP, 0.5 units of EX Taq polymerase and 375 μM $MgCl_2$. Amplification conditions were: denaturation at 95°C for 2 min followed by multiple cycles of 95°C for 15 s and 68°C for 30 s.

At the end of the last extension phase, the temperature of the reaction mixture was raised from 50 to 95°C at a rate of 0.2°C per second. Within a specific temperature range, typically between 87 and 92°C, the primer dimer was denatured and became single-stranded, whereas the target PCR product remained double-stranded. Fluorescent signals measured

Table 1 Polymerase chain reaction primers used for amplification

Gene	Forward primer	Reverse primer	Size (bp)
HOXA1	CGCGTTAAATCAGGAAGCAGAC	CAAAAGTCTGCGCTGGAGAAGATG	286
HOXA2	GACCATTCCCAGCCTGAACC	GTCTCTCAGTCAAATCCAGCAGC	397
HOXA3	CTCACCCACAGTGGCCAAAC	GTACTTCATGCGGCGATTCTGG	300
HOXA4	GACACCGCCTACCCCTATG	CTCCTTCTCCAGCTCCAAGAC	413
HOXA5	CCACATCAGCAGCAGAGAGG	GTCAGGTAACGGTTGAAGTGGAAC	260
HOXA6	CCTGCACTTTTCTCCCGAGC	GCGTTGGCGATCTCGATGC	269
HOXA7	CCTTCGCCTCGACCGTTC	GTAGCGGTTGAAGTGGAACTCC	328
HOXA9	CTAGAGAGAAAAAGAAAGAACTGTCCGTC	CAAGCTAACACACACAGCTATCAGC	255
HOXA10	TCCTGATGAATCTCCAGGCGAC	AGCCCTGCACAGATGTAACGG	160
HOXA11	GCGCCGGCAACTTCAAGTTC	GATTTTGACTTGACGATCAGTGAGGTTG	308
HOXA13	GGAACGGCCAAATGTACTGCC	CCGCCTCCGTTTGTCCTTAG	211
HOXB1	CACCCTGCCCTTCAGAACC	CTGTGTTTCATTGAGCTCCAGGG	244
HOXB2	GCCAAAAGCGAGCCGAAGATGG	GCAGCTGCGTGTTGGTGTAAG	266
HOXB3	GAGTCGAGGCAAACGTCCAAG	CTCGCTGAGGTTCAGCAGG	287
HOXB4	CCTGGATGCGCAAAGTTCACG	GATCTTGGTGTTGGGCAACTTGTG	259
HOXB5	GGATGAGGAAGCTTCACATCAGC	CAGCTGTAGCCAGGCTCATAC	257
HOXB6	GGATGAATTCGTGCAACAGTGAGTG	GGGACTTTGCAAACTTTGTAACTCCTG	224
HOXB7	CCCTTTGAGCAGAACCTCTCC	GAGCGTGTGCGCGATCTC	254
HOXB8	GCAGTACGCAGACTGCAAGC	GACCTGTCTCTCTGTCAGTC	258
HOXB9	GCTGCTCAAACAGGGCACG	GGTCCCTGGTGAGGTACATATTG	262
HOXB13	CAAGGTGAAGAACAGCGCTACC	TCCTGAGGAACAGTCCAGCAG	184
HOXC4	GCCAGCAAGCAACCCATAGTC	GTGCTGACCTGACTTTGGTGTTG	198
HOXC5	GAGCGAGCTAAGAGCAGTGG	CACAAGTTGTTGGCGATCTCTATGC	252
HOXC6	GGACCAGAAAGCCAGTATCCAG	CTGTCGCTCGGTCAGGC	213
HOXC8	CACTAACAGTAGCGAAGGACAAGG	GACTTCAATCCGACGTTTTCGTGTC	192
HOXC9	GGACTACATGTACGGCTCGC	GAAGAGAAACTCCTTCTCCAGTTCC	225
HOXC10	GAAATCAAGACGGAGCAGAGCC	CCAGCGTCTGGTGTTTAGTATAGG	210
HOXC11	CTGAGGAGGAGAACACAAATCCC	GTTGAAGAAAAACTCTCGCTCCAGTTC	163
HOXC12	CCAGTCGCTGGAATCCGAC	GCTCTGCCAGTTGCAACTTCG	243
HOXC13	GCACTGGGCTCTCTCCAATG	CTCTTTGGTGATGAACTTGCTAGCC	222
HOXD1	CCTTCAGCACGTTCGAGTGG	CAAGCAGTTGGCTATCTCGATGC	199
HOXD3	TGGAGTGCCTGCCAAGAAGC	CGTTCCGTGAGATTCAGCAGG	302
HOXD4	GCTCCAGGAGAGCCTTGC	GACAGACACAGGGTGTGAGC	313
HOXD8	CGGATACGATAACTTACAGAGACAGC	GTCTTCCTCTTCGTCTACCAGG	296
HOXD9	GATCCCAGGCTGTTCGCTGAA	GTTAGGTTGAGAATCCTGGCCAC	230
HOXD10	GAGGTCTCCGTGTCCAGTC	CCTGTCGGTGAGGTTAACGC	227
HOXD11	GCAGTCCCTGCACCAAGG	GGTTGAGCATCCGAGAGAGTTG	251
HOXD12	CCTGGCTTCAAGGACGACAC	CCTTGCGTTTCTGCCTGTTGATG	253
HOXD13	CATGGTGTCCACTTTCGGCTC	CTCGTTCTCCAGTTCTTTAAGCTGC	261

within this temperature range reflect the target PCR products because SYBR Green binds to double-stranded DNA but not to single-stranded DNA (Morrison *et al.* 1998). The threshold cycle (C_T) was defined as the number of cycles at which the fluorescent value was first detected.

Standard curve generation and sample measurement

A serial dilution of PCR product ranging from 10 copies/μL to 10^8 copies/μL was re-amplified by real-time PCR to determine the threshold cycle (C_T). Sample cDNA were prepared from Human Digestive System MTC panel (BD Bio-

Table 2 Source used for each of the *Hox* genes

Gene	Source	Gene	Source	Gene	Source	Gene	Source
HOXA1	FB	*HOXB1*	FB	*HOXC4*	Spleen	*HOXD1*	FB
HOXA2	FB	*HOXB2*	FM	*HOXC5*	FSI	*HOXD3*	FB
HOXA3	FSI	*HOXB3*	Lung	*HOXC6*	FM	*HOXD4*	FB
HOXA4	FM	*HOXB4*	FM	*HOXC8*	FM	*HOXD8*	FB
HOXA5	FSI	*HOXB5*	AGM	*HOXC9*	FM	*HOXD9*	AGM
HOXA6	FB	*HOXB6*	FM	*HOXC10*	FM	*HOXD10*	AGM
HOXA7	FB	*HOXB7*	AGM	*HOXC11*	AGM	*HOXD11*	AGM
HOXA9	AGM	*HOXB8*	AGM	HOXC12	Leukocyte	*HOXD12*	FM
HOXA10	AGM	*HOXB9*	AGM	*HOXC13*	FM	*HOXD13*	FM
HOXA11	AGM	*HOXB13*	AGM				
HOXA13	AGM						

Different sources were used: Fetal mix (FM); fetal brain (FB); fetal small intestinal (FSI); adult GI mix (AGM); lung, spleen and leukocyte.

sciences Clontech, Palo Alto, CA, USA), derived from full thickness tissue, and 0.2 ng of each cDNA was used for *Hox* gene expression analysis. C_T values were plotted against log values of the initial copy numbers. The initial copy number of the sample was determined by extrapolating the C_T values from the standard curve. All measurements were performed in triplicate.

The copy number of the *Hox* gene was divided by the copy number of *GAPDH*, a ubiquitously expressed housekeeping gene, to normalize the tissue materials from which the cDNA was derived (Karge *et al.* 1998). This ratio is referred to as the *HOX-GAPDH* ratio in the sections below.

Statistical analysis

All statistical analyzes were performed using the mathematical functions of the S-PLUS computer language (Insightful, Seattle, WA, USA). Repeated-measures analysis was performed using the *lme* function (Pinheiro & Bates 2000). The overall *Hox* expression data was summarized as a data matrix with the rows representing the 39 *Hox* genes and with the columns representing the anteroposterior positions along the GI tract. The data matrix was scaled and centered with the *scale* function of the S-PLUS package so that each row would have a mean of zero and a standard deviation of one. The data matrix was transformed into the principal components space based on the scaled correlation matrix by using the *princomp* function. The results were expressed as a biplot (Gabriel 1971) by using the *biplot.princomp* function.

Permax analysis (Mutter & Lea 2001) was performed to discriminate genes expressed in the foregut-derived segments, midgut-derived segments, and hindgut-derived segments. The Wilcoxon statistics of the 39 *Hox* genes were computed for each attribute (i.e. expression profile along the anteroposterior axis of the GI tract). The degree of significance was assessed based on the permutation distribution of the maximum and minimum over all attributes by the *permax* function (Cox 1974). The results were displayed graphically using the *permax.plot* function.

The expression level of a particular *Hox* gene at a particular position along the GI tract, z, was regarded as a function of the paralogous number x and anatomical position y. The three dimensional data sets: x; y; and z; were fitted onto a trend surface by the least squares method to the fourth order polynomials by using the *surf.ls* function.

RESULTS

Reproducibility of the real-time PCR assay

Approximately 10^8 copies/μL of cDNA were serially diluted seven orders of magnitude down to 10 copies/μL, and each of the dilution was subjected to real-time PCR. The C_T values, as defined in the methods section, were then plotted against the log values of the initial amounts of template. The correlation coefficients for the standard curves of each *Hox* gene were all above 0.95, ranging from 0.96 to 0.999.

Expression pattern along the anteroposterior axis

The expression level of all 39 *Hox* genes along the GI tract (full thickness) is depicted in Fig. 1. *Hox* gene expression level was dependent on three parameters: (1) anteroposterior position along the GI tract (e.g. esophagus through rectum); (2) paralog cluster (e.g. *HOXA* through *HOXD*); and (3) paralog position (e.g. 1 thorough 13).

The biplot representation of the principal coordinates (Fig. 2) revealed that the vectors representing the expression

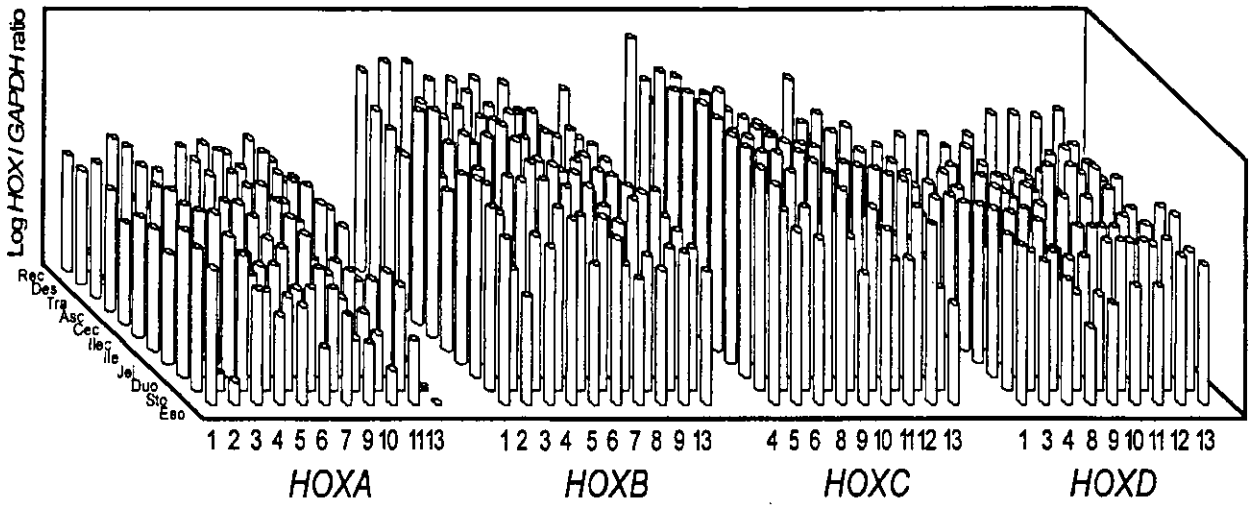

Fig. 1 Overall expression pattern of 39 *HOX* genes. The *x*-axis denotes 39 *HOX* genes, the *y*-axis denotes the anteroposterior (GI tract. Eso, esophagus; Sto, stomach; Duo, duodenum; Jej, jejunum; Ile, ileum; Ilec, ileocecum; Cec, cecum; Asc, ascending colon; Tra, transverse colon; Des, descending colon; Rec, rectum), and the *z*-axis denotes the expression level (ratio of *HOX* gene copy number/ *GAPDH* copy number was logarithmically transformed).

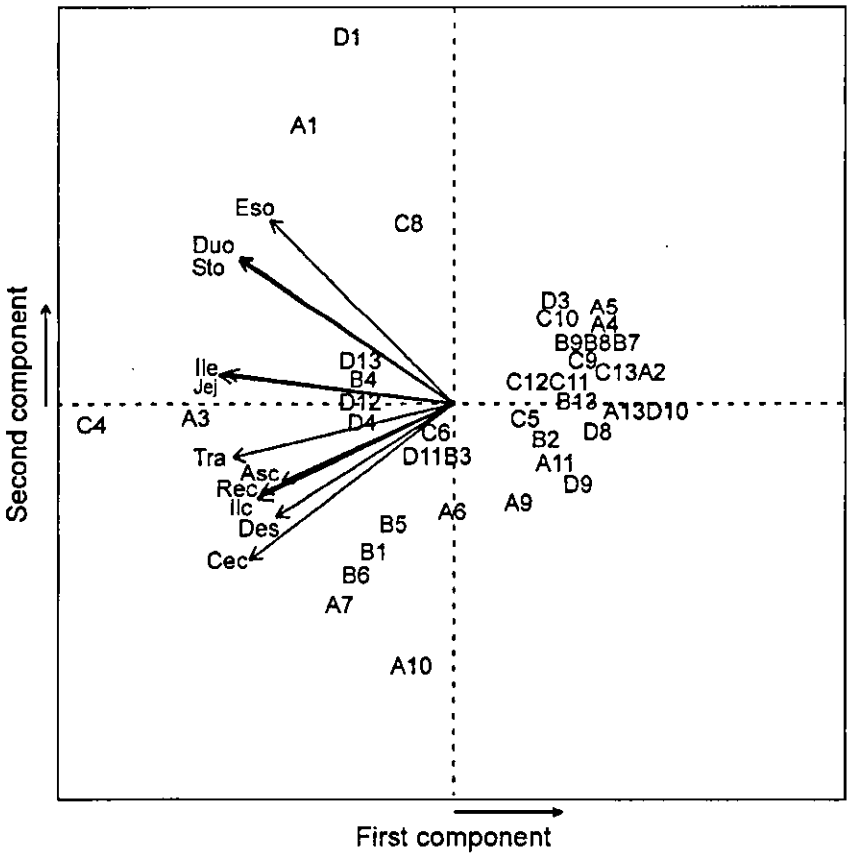

Fig. 2 Biplot of the 39 *Hox* genes and tissues by principal components analysis. This model shows a two-dimensional correlation between *Hox* genes and tissues. In this model, the *Hox* genes profile and tissues are represented by their location; *Hox* gene subsets are represented by their respective numeric symbol. The correlations between the tissues (Eso, esophagus; Sto, stomach; Duo, duodenum; Jej, jejunum; Ile, ileum; Ilec, ileocecum; Cec, cecum; Asc, ascending colon; Tra, transverse colon; Des, descending colon; Rec, rectum) are represented by the cosines of the angles between the arrows.

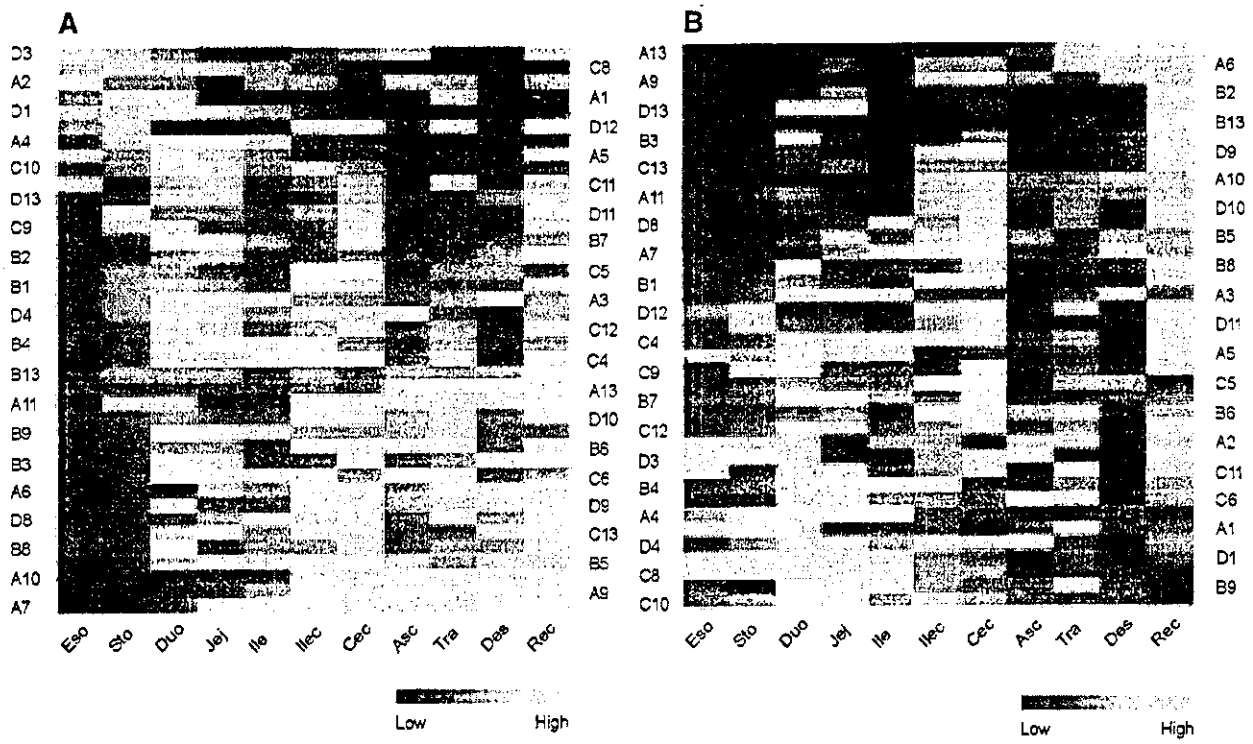

Fig. 3 Permax view of the expression levels of 39 *HOX* genes in 11 GI tract tissues. The gene expression levels in the hindgut discriminated it from the foregut and midgut. Gene expression levels are color-coded according to the key. The highest expression level is colored bright yellow, and the lowest is colored red. **A:** View of the foregut-based and midgut-based expression pattern. **B:** View of the hindgut-based expression pattern.

pattern of the *Hox* genes in the tissues derived from the foregut (i.e. esophagus and stomach) share comparable lengths and directions. Similarly, vectors representing the expression pattern of *Hox* genes in the tissues derived from the midgut (i.e. duodenum, jejunum, ileum, ileocecum, cecum, ascending colon and transverse colon) and the hindgut (descending colon and rectum) exhibited comparable lengths and directions.

Permax analysis (Mutter 2001) was used to discriminate genes expressed in the hindgut (descending colon and rectum) from those expressed in the foregut or midgut (Fig. 3). The *permax.plot* graphical results revealed that *Hox* genes with high expression in the foregut tended to have low expression in the hindgut, whereas those with low expression in the foregut tended to have high expression in the hindgut. More specifically, a subset of genes (i.e. *HOXD3*, *HOXC8*, *HOXA2*, *HOXA1*, *HOXD1*, *HOXD12*, *HOXA4*, *HOXA5*, *HOXC10*, *HOXC11*) was expressed at a higher level in the foregut region (Fig. 3A), and a subset of genes (i.e. *HOXA13*, *HOXA6*, *HOXA9*, *HOXB2*, *HOXD13*, *HOXB13*, *HOXB3*, *HOXD9*, *HOXC13*, *HOXA10*) was expressed at a higher level in the hindgut region (Fig. 3B), paralog 13 (*HOXA13*, *HOXB13*, and *HOXD13*) tended to be more highly expressed in the hindgut region than paralogs 9 through 12.

Plotting of the expression level of each *Hox* cluster as a function of the paralog number and relative position along the anteroposterior axis revealed distinctive patterns for the trend surfaces of each cluster (Fig. 4). *HOXA*: The trend surface had two peaks, at coordinate positions (A1, 1; and A9, 11). Moderate expression levels were observed between the ileocecum and cecum. A monotonic decrease was observed at *HOXA1* through *HOXA3*, whereas a monotonic increase was observed at *HOXA4* through *HOXA10*. Genes with a high level of expression at the foregut tended to have a low level of expression in the hindgut region, whereas those with a low level of expression in the foregut region tended to be highly expressed in the hindgut region. Although the expression level was low at *HOXA13*, the peak in the rectum was high.

HOXB

HOXB1 through *HOXB3* had especially high expression peaks in the midgut region. A monotonic decrease was observed at *HOXB4* through *HOXB9*. Although the expres-